Classification Based Approach for Spectral Signature of Remotely Sensed Temporal Data

H.Farouk† and B.M.Abdel Latif††

† Egyptian Environmental Affairs Agency, Egypt.
†† National Authority for Remote Sensing & Space Sciences, Egypt.

Summary
Techniques based on multi-temporal, multi-spectral and satellite-sensor have demonstrated potential as a means to detect, identify, map and monitor ecosystem changes. Multi-temporal images processing becomes more and more important in monitoring earth surface. The large collection of past and present remote sensing imagery makes it possible to analyze spatio-temporal and spectro-temporal pattern of environmental elements. However most existing multi-temporal classification methods use the spectral information alone, ignoring the spatial and temporal correlation between images acquired from different dates, in spite of this represents an amount of information far greater than the individual images. However, their analysis is complex and difficult. This enables to extract evolutions of the same geographic area over time to create a generic spectral signature. In this paper a database of spectral signatures was created for the three main features of the earth; water, vegetation and soil. As large free archives of Landsat 7 ETM+ has been created over time. A temporal series of Landsat 7 ETM+ scenes of different training sites were used to extract the spectral signatures in a reflectance representation by accumulating the individual signatures collected form the individual scenes. The signatures are collected in a statistics form; the mean, minimum, maximum and standard deviations of the training pixels values in the reflectance representation. The database was developed as windows application. Searching has been included to allow users quickly search for the signature of interest. The database was only filled by Landsat 7 ETM+ signatures for the three main features of the earth; water, vegetation and soil which are the features of interest of this study, but it is designed to accommodate other spectral signatures of different satellites and features. Temporal series of Landsat 7 ETM+ scenes of five different lakes located in Egypt are used. The first lake is Burullus Lake at path 177 and raw 38 located in the Nile Delta. The second lake is Qaroun Lake at path 177 and raw 40 located in Fayoum governorate. The third lake is Nasser Lake at path 174 and raw 44 located in Aswan governorate. The selected lakes are typical areas that represent the three main features of the earth. They typically include water, vegetation and soil. That's why they are selected as study areas. All images are converted to reflectance representation form in order to be independent of the illumination and atmospheric characteristics. In this paper a new spectral classification method is introduced based on the spectral signature database. The classification process is done based on the mean, minimum and maximum of the spectral signature from the database. This paper introduces classification for only the three main classes of the earth; water, vegetation and soil for only Landsat 7 ETM+. However, it is supposed that, classification of any other feature for any other satellite can similarly be done after extracting its corresponding spectral signature and filling in the spectral signature database. A series of tests was applied on the same scenes but with different date to extract the three main classes; water, vegetation and soil. Accuracy assessment has proven that the introduced classifier that uses the spectral signature gives nearly the same results of the supervised classification that uses the signature that was extracted from each image individually. It is supposed that any classifier that uses the proposed spectral signature should give better results than using the individual signature extracted from a single image that is to be classified. Moreover, it is supposed that, the more enhanced classifiers should give better classification results than the introduced classifier.

Key words:
Classification, Spectral Signature, Signature Database, Satellite Images and Landsat.

1. Introduction

When an electromagnetic strikes a target surface, three interactions are possible: reflection, transmission and scattering. It is the reflected radiation, generally modeled as reflectance that is measured by the remote sensor. For any given material, the amount of solar radiation that is reflected (absorbed, transmitted) will vary with wavelength. It is, in fact, the wavelengths that are not returned to the sensor that provide information about the imaged area [1]. Every material has a characteristic spectrum based on the chemical composition of the material. When sunlight strikes a target, certain wavelengths are absorbed by the chemical bonds; the rest are reflected back to the sensor. This important property of matter, whether the target is mineral, vegetation, man-made, or even the atmosphere itself, allows to separate distinct cover types based on their response values for a given wavelength. When we plot the response characteristics of a certain cover type against wavelength, we define what is termed the spectral signature of that cover. Fig. 1 illustrates the spectral signatures for some common cover types for Landsat 7 ETM+, Landsat 5 TM and Landsat 4 MSS.

By overlapping the spectral curves from different features you can see how well different sensors provide information about the feature's spectral curve. By comparing the response patterns of different features we may be able to distinguish between them, where we might not be able to, if

Manuscript received November 5, 2013
Manuscript revised November 20, 2013

we only compared them at one wavelength. Spectral response can be quite variable, even for the same target type, and can also vary with time (e.g. "green-ness" of leaves) and location. Knowing where to "look" spectrally and understanding the factors which influence the spectral response of the features of interest are critical to correctly interpret the interaction of electromagnetic radiation with the surface.

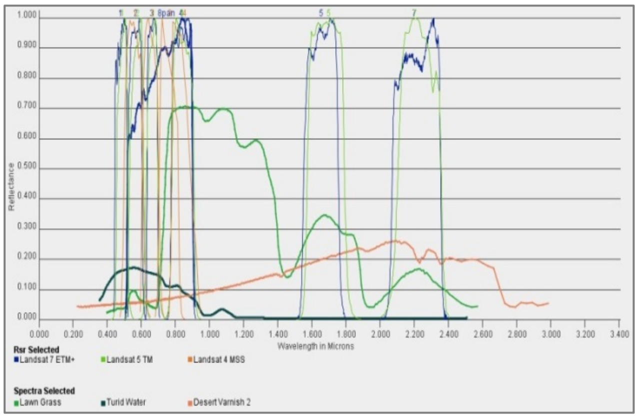

Fig. 1 The spectral signatures for some common cover types for Landsat 7 ETM+, Landsat 5 TM and Landsat 4 MSS (Source: USGS).

Remotely sensed data are made up of reflectance values. The resulting reflectance values translate into discrete digital numbers (or values) recorded by the sensing device. These gray scale values fit within a certain bit range (such as 0 to 255, which is 8-bit data) depending on the characteristics of the sensor. The fundamental task in remote sensing is distinguishing objects on earth, based on the amount of light that objects reflect across the various wavelengths that satellites measure (captured in bands). The problem is that satellites don't directly measure reflectance, they measure radiance. The pattern of radiance across the satellite bands is often similar to the pattern of reflectance across the same bands, but at-satellite radiance is altered by atmospheric effects because the light going to and reflecting off the ground goes through the atmosphere before reaching the satellite. Another issue is that it is often needed to directly compare the reflectance of objects measured on the ground with reflectance calculated from satellite data. So, it is a must to convert satellite digital numbers (DNs), or pixel values, to ground reflectance [2]. Spectral reflectance is the efficiency by which a material reflects energy as a function of wavelength. Unfortunately, the problem is not as simple as it may appear since other factors beside the sensor play a role; such as solar angle, view angle, surface wetness, and background and surrounding material. Another problem is that we have to deal with the fact that the energy often measured by the sensor will be from a mixture of many different materials.

With knowledge of the spectral reflectance characteristics of the earth cover types; we can identify and map them in areas we are generally unfamiliar with. Provided with a multi-spectral image of an area; even though we are totally unfamiliar with, we can identify the dominant cover types with a high degree of certainty, by utilizing our knowledge about the spectral characteristics of certain surface materials (spectral signatures). The spectral signature is the information that is used in classifying pixels in an image. Because of this primary role of spectral signatures, efforts have been made over the past decade to compile databases, termed Spectral Libraries, of the spectra of known materials [3]. These libraries include human-made materials, pure minerals, site-specific minerals, pure vegetation stands, and various mixed-composition spectra. Many of these libraries are available to the public or selected researchers like USGS Digital Spectral Library 06.

Techniques based on multi-temporal, multi-spectral and satellite-sensor acquired data have demonstrated potential as a means to detect, identify, map and monitor ecosystem changes, irrespective of their causal agents [4]. However most existing multi-temporal classification methods use the spectral information alone, ignoring the spatial and temporal correlation between images acquired from different dates [5], in spite of this represents an amount of information far greater than individual images. However, their analysis is complex and difficult. This enables us to try to extract evolutions of the same geographic area over time, creating satellite image time series and creating a generic spectral signature.

One of the most common requirements in and an important part of remote sensing and image analysis is classification. It is the need to segment or classify an image into land cover, material, or object classes. In some cases, this is an end in itself [6] and objective of the analysis. The analyst must select a classification method, i.e. a classifier that will best accomplish a specific task. At present, it is not possible to state which classifier is best for all situation as the characteristic of each image and the circumstances for each study vary so greatly. Therefore, it is essential that each analyst understand the alternative strategies for image classification so that he or she may be prepared to select the most appropriate classifier for the task in hand [7][8].

In this paper, a new classification technique is introduced for any given areas that we are totally unfamiliar with by using a generic spectral signature. However, this technique was only tested for the three main classes of the earth; water, vegetation and soil for only Landsat 7 ETM+. However, it is supposed that, classification of any other feature for any satellite can similarly be done after extracting its corresponding spectral signature.

Fig. 2 shows the reflectance pattern of the three main features of the earth. The characteristics of these features can be summarized as follows;

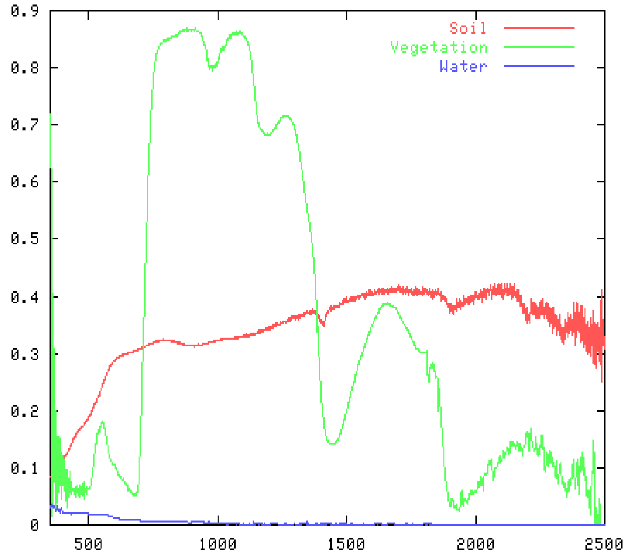

Fig. 2 The reflectance pattern of water, vegetation and soil. (Source: http:\\www.uwyo.edu\rs4111\le10_veg_index1_f12.pptx)

Water - Longer wavelength visible and near infrared radiation is absorbed more by water than shorter visible wavelengths. Thus water typically looks blue or blue-green due to stronger reflectance at these shorter wavelengths, and darker if viewed at red or near infrared wavelengths. If there is suspended sediment present in the upper layers of the water body, then this will allow better reflectivity and a brighter appearance of the water. Suspended sediment can be easily confused with shallow (but clear) water, since these two phenomena appear very similar. Chlorophyll in algae absorbs more of the blue wavelengths and reflects the green, making the water appear more green in colour when algae is present. The topography of the water surface (rough, smooth, floating materials, etc.) can also lead to complications for water-related interpretation due to potential problems of specular reflection and other influences on colour and brightness [9].

Vegetation - A chemical compound in leaves called chlorophyll strongly absorbs radiation in the red and blue wavelengths but reflects green wavelengths. Leaves appear "greenest" to human eye in the summer, when chlorophyll content is at its maximum. In autumn, there is less chlorophyll in the leaves, so there is less absorption and proportionately more reflection of the red wavelengths, making the leaves appear red or yellow (yellow is a combination of red and green wavelengths). The internal structure of healthy leaves act as excellent diffuse reflectors of near-infrared wavelengths. If our eyes were sensitive to near-infrared, trees would appear extremely bright to us at these wavelengths. In fact, measuring and monitoring the near-IR reflectance is one way that scientists can determine how healthy (or unhealthy) vegetation may be [9].

Soil - Soils tend to have reflection properties that increase approximately monotonically with wavelength. They tend to have high reflectance in all bands. This of course is dependent on factors such as the colour, constituents and especially the moisture content. As described above, water is a relatively strong absorber of all wavelengths, particularly those longer than the red part of the visible spectrum. Therefore, as soils moisture content increases, the overall reflectance of that soil tends to decrease. Soils rich in iron oxide reflect proportionally more of the red than other visible wavelengths and therefore appear red (rust colour) to the human eye. A sandy soil on the other hand tends to appear bright white in imagery because visible wavelengths are more or less equally reflected; when slightly less blue wavelengths are reflected this results in a yellow colour [9].

2. Data Sources and Selection Criteria

Landsat Multispectral data provide the longest duration archive of moderately high spatial resolution satellite image data for monitoring the types and rates of land-surface change imposed by human activity. That's why several Landsat 7 ETM+ images are selected for

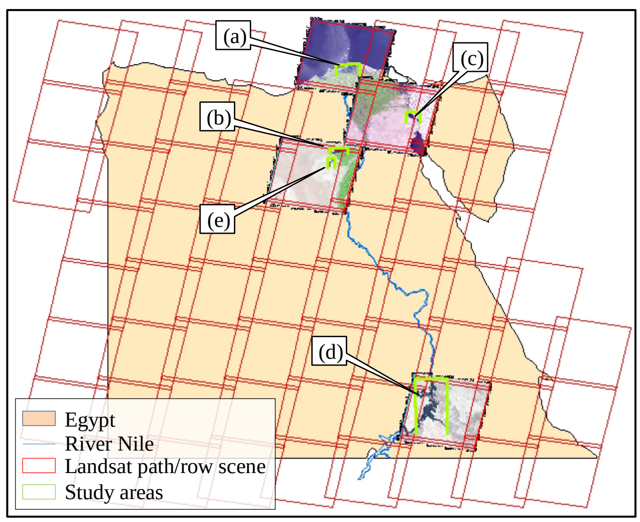

Fig. 3 Egypt map showing the study areas.
(a) Burullus Lake (b) Qaroun Lake (c) Morra Lakes
(d) Nasser Lake (e) Rayan Lakes

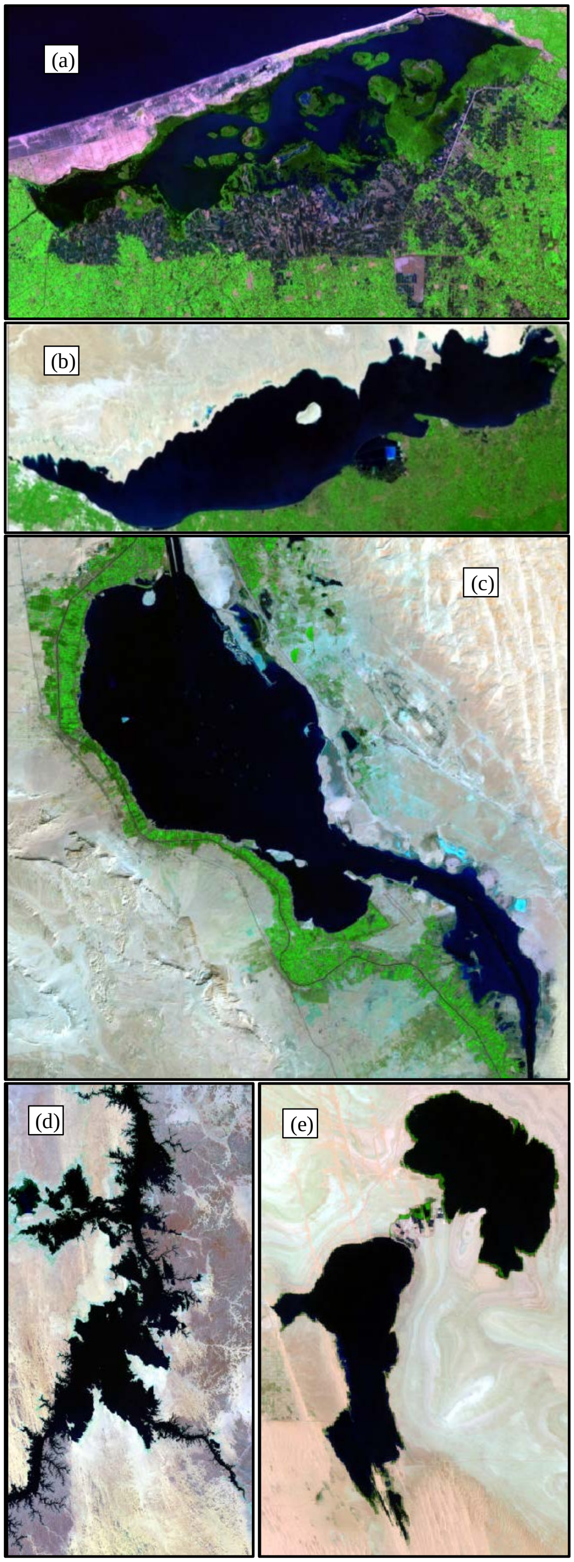

Fig 4: Natural-color composite bands 7,4,2 of Landsat 7 ETM+ of (a) Burullus Lake (b) Qaroun Lake (c) Morra Lakes (d) Nasser Lake (e) Rayan Lakes

Processing in this study. Surveys proved that years 2002 and 2003 have a reasonable number of scenes that are available online and clouds-free of the selected sites of study. That's why these dates are used. Temporal series of four scenes of five different lakes located in Egypt are used as shown in Fig. 3. Three of each series for each lake were used for extracting the spectral signature and the fourth image was used for testing the extracted spectral signatures that were stored in the spectral signature database. The selected lakes are typical areas that represent the three main features of the earth. They typically include the features; water, vegetation and soil. That's why they are selected as training areas of this study. Table 1 shows the metadata of used images. Snapshots of these study areas are shown in Fig 4.

Table 1: Metadata of used Landsat 7 ETM+ scenes of the study areas.

Study Area	*Path, Row*	*Serial*	*Scene Name*	*Image Date*
Burullus	P177, R38	1	LE71770382003107ASN00	2003-04-17
		2	LE71770382003027SGS00	2003-01-27
		3	LE71770382003011SGS02	2003-01-11
		4	LE71770382002168EDC00	2002-06-17
Qaroun and Rayan	P177, R40	1	LE71770402003123ASN00	2003-05-03
		2	LE71770402003059SGS00	2003-02-28
		3	LE71770402003027SGS00	2003-01-27
		4	LE71770402003011SGS02	2003-01-11
Nasser	P174, R40	1	LE71740442003118ASN00	2003-04-28
		2	LE71740442003070SGS00	2003-03-11
		3	LE71740442003038SGS00	2003-02-07
		4	LE71740442003022SGS00	2003-01-22
Morra	P176, R39	1	LE71760392003068SGS00	2003-03-09
		2	LE71760392003036SGS00	2003-02-05
		3	LE71760392002353SGS00	2003-12-19
		4	LE71760392002305SGS00	2002-11-01

The first lake is Burullus lake at path 177 and raw 38 located in the Nile Delta. The second and the third lake is Qaroun lake and Rayan lakes located at path 177 / raw 40 located in Fayoum governorate. The fourth lake is Nasser lake located at path 174 / raw 44 located in Aswan governorate. The last and fifth lake is El-Morra lakes located at path 176 / raw 39 located on Suez Canal in Suez governorate.

All these images have been downloaded from USGS using Earth Explorer and Glovis web applications. All image processing has been processed by using the ERDAS Imagine 2013 and ArcGIS 10.2 software.

3. Methodology

The flow chart in Fig. 5 summarizes the steps of the introduced classifier. All images were preliminarily geometrically and radiometrically corrected. Then, image to image registration was done for all used images of the same location. Keeping the root mean square error (RMSE) less than 0.5 pixels, an image to image transformation model (third order polynomial) and nearest neighbor resampling was calculated. All images are converted to reflectance in order to be independent of the illumination and atmospheric characteristics. The second step is to extract the spectral signature and filling in the pre-created spectral signature database. The final step is the classification of images with recoding which is done using the spectral signature form the spectral signature database.

3.1 Signatures Extraction

Signatures were taken as a group of pixels as polygons for the three main classes of earth; water, vegetation and soil. Collection of polygons was precisely taken from scenes for the three features of interest to collect their spectral signatures. Signatures are collected as statistics of the training pixels values; the mean, minimum, maximum and standard deviations as reflectance representation. As mentioned above, the reflectance values were used in order to be independent of the illumination and atmospheric characteristics. Graphs for the signatures mean were plotted for all training set for each signature for each scene in order to ensure the homogeneity of the taken signatures.

Feature space images were created in order to ensure the disjoint of the signatures for the three features of interest after aggregation. In fact, band 4 versus band 5 feature space shows disjoint classes for water and vegetation. In addition, band 5 versus band 7 feature space shows disjoint classes for water and soil. For example, Fig. 6 shows disjoint classes for Burullus lake image dated 11-01-2003. The drawn ellipses on the feature space images in Fig. 6 represent the pixels assigned to each class according to the

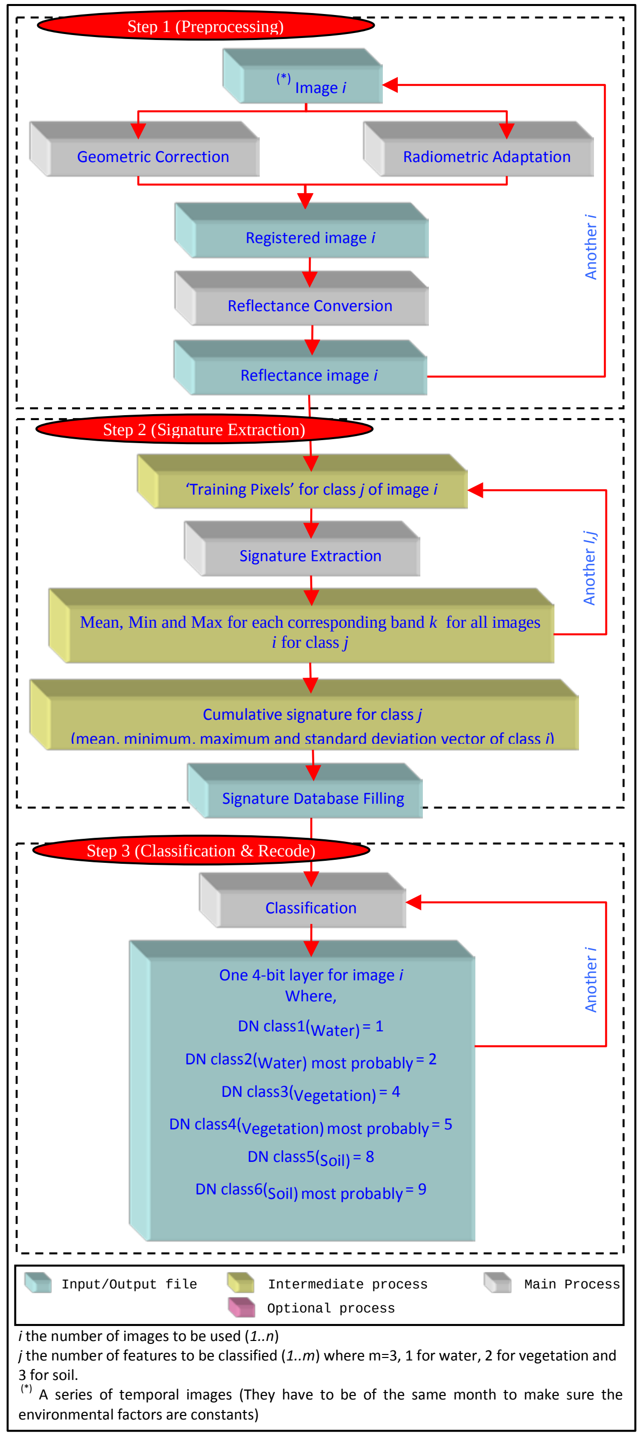

Fig. 5 Flow chart of the introduced classifier that uses the proposed spectral signature of the three classes; water, vegetation and soil.

signature statistics. Clearly there are a lot of gaps in the feature space plot that should be filled in with additional training sites. However, this study is interested in only the three main features of the earth; water, vegetation and soil. In most classification projects dozens of training areas are defined to eliminate the large gaps between objects in feature space. The following table summarizes the spectral signature for the three main classes of the earth; water, vegetation and soil that were stored in the signature database for Landsat 7 ETM+.

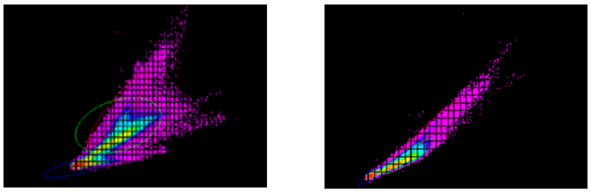

Band#4 vs Band#5 Band#5 vs Band#7

Fig. 6 Feature space for Burullus lake dated 2003-01-11.
Blue, green and red ellipses represent water, vegetation and soil respectively.

Table 2: Statistics of the proposed water, vegetation and soil signatures.

		Min	*Max*	*Mean*	*St.Dev.*
Band1	***Water***	0.084	0.363	0.109	0.015
Band2		0.05	0.398	0.08	0.02
Band3		0.026	0.415	0.055	0.021
Band4		0.006	0.32	0.041	0.025
Band5		0.018	0.14	0.021	0.016
Band7		0.019	0.113	0.016	0.012
Band1	***Vegetation***	0.09	0.218	0.122	0.012
Band2		0.061	0.258	0.105	0.016
Band3		0.042	0.312	0.093	0.026
Band4		0.047	0.585	0.2	0.09
Band5		0.001	0.384	0.125	0.038
Band7		0.012	0.269	0.078	0.031
Band1	***Soil***	0.101	0.395	0.182	0.021
Band2		0.077	0.482	0.219	0.039
Band3		0.064	0.611	0.291	0.069
Band4		0.087	0.736	0.346	0.085
Band5		0.001	1.177	0.43	0.101
Band7		0.031	1.125	0.357	0.09

Then for all scenes of different dates of all lakes, the signatures were combined and aggregated into one single signature for each class. Table 2 shows the statistics of each class. Fig. 7 shows the spectral signature profile for the signature mean numbers of the three classes after aggregation. Tests, that can help determine whether the signature data are a true representation of the classes of interest, were performed. Transformed divergence of equation Eq. 1 is a measure of the signature separability that gives results greater than 1900 which means that the classes of these signatures can be well separated [1].

$$D_{ij} = \frac{1}{2}\mathrm{tr}((C_i - C_j)(C_i^{-1} - C_j^{-1})) + \frac{1}{2}\mathrm{tr}((C_i^{-1} - C_j^{-1})(\mu_i - \mu_j)(\mu_i - \mu_j)^T) \qquad (1)$$

Where:
D_{ij} = Divergence between two signatures (classes)
i and j = the two signatures (classes) being compared
C_i = the covariance matrix of signature i
μ_i = the mean vector of signature i
tr = the trace function (matrix algebra)
T = the transposition function

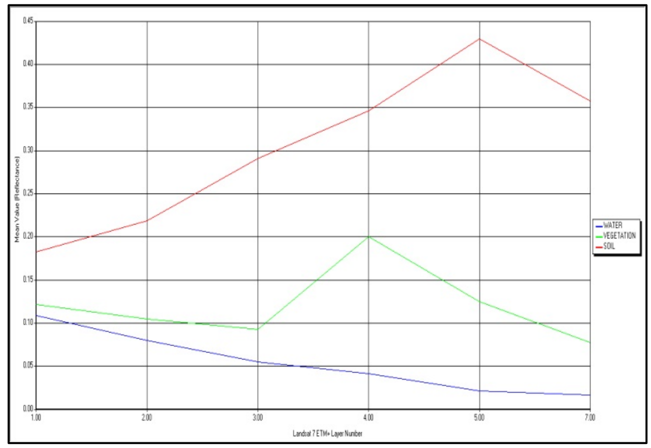

Fig. 7 Spectral signature profile for the signature mean numbers of the three classes after aggregation.

3.2 Database

The extracted signatures were stored in a database. The entity relationship diagram (ERD) of the spectral signature database is shown in the following Fig 8. The database was developed in a stand-alone version using Microsoft Access 2013 and Visual Basic for Applications (VBA). Searching has been added to the database GUI to allow users quickly search for the signature of interest. Since the used images were from the Landsat 7 ETM+. So the signatures that were entered in the database were only for Landsat 7 ETM+ for the water, vegetation and soil signatures only. However the database was designed to store the signatures for any other features from any other platforms which needs an extra work and was leaved to future work

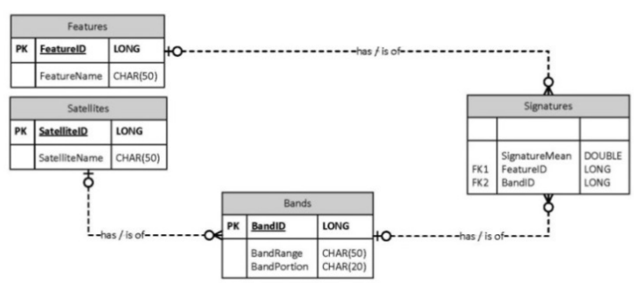

Fig 8 The entity relationship diagram (ERD) of the spectral signature database.

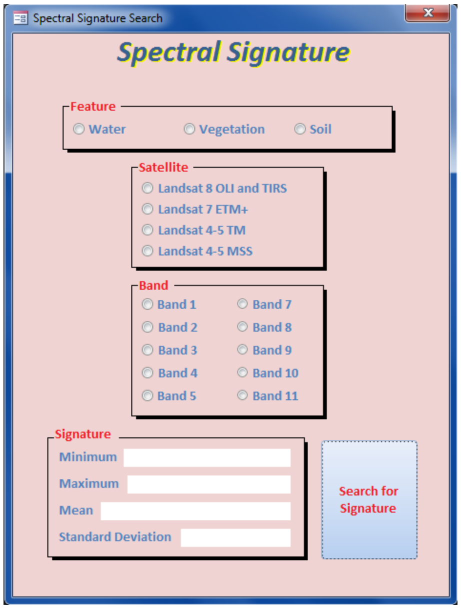

Fig. 9 A snapshot of the main database GUI for searching the signature of interest.

research. A snapshot of the main interface for the database for searching is shown in the Fig. 9. The data stored in the database are;

- Feature Name (datatype: text) for which a signature is extracted (e.g. Water, Vegetation, Soil, …)
- Platform Name (datatype: text) of the image (e.g. Landsat 7 ETM+, …)
- Band Number (datatype: text) for which a signature is extracted (e.g. Band1, Band2, Band3, …)
- Signature (datatype: number-float) in a form of digital numbers for the mean, minimum, maximum and standard deviation of the training pixels DN values in the reflectance representation.

3.3 Classification

The statistics of the signatures, which were stored in the spectral signature database, are used to determine which pixel is closest to. Each pixel in the image is compared to the signatures of the three main classes of the earth; water, vegetation and soil that have been defined in the spectral signature database. The pixel's class assignment is determined by the "closest" mean vector based on the minimum distance classifier in Eq. 2. Fig. 10 simplifies the idea. It shows a three-band multispectral image pixel *p* as a vector in three-dimensional space and the three objects of interest; water, vegetation and soil that have been defined on a three-band multispectral feature space plot. The boxes represent the pixels assigned to each object. The intent of the introduced classifier is to find which object, *p* belongs to. However, the dimension of the introduced classifier is six-dimensional that represents band1, band2, band 3, band4, band5 and band7 of Landsat 7 ETM+. Trivially, the thermal bands; band 61 and band 62 are not included in the calculation.

$$SD_{xyc} = \sqrt{\sum_{i=1}^{n} \left(\mu_{ci} - X_{xyi}\right)^2} \qquad (2)$$

Where:
n = number of bands (dimensions)
i = a particular band
c = a particular class
X_{xyi} = data file value of pixel x, y in band i
μ_{ci} = mean of data file values in band i for the sample for class c
SD_{xyc} = spectral distance from pixel x, y to the mean of class c

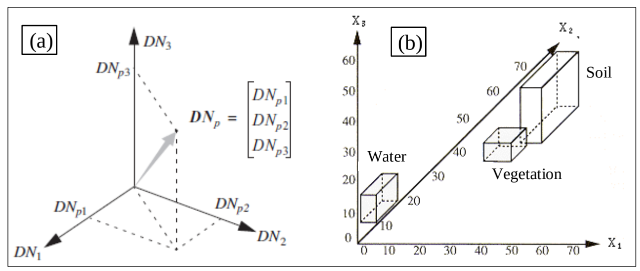

Fig. 10 (a) Pixel vector *p* represented in a three-dimensional space. (b) Three objects of interest; water, vegetation and soil on a three-band multispectral feature space plot.

The introduced classifier classifies the image into six classes; [i]water (coded 1 and colored blue), [ii]most probably water (coded 2 and colored blue), [iii]vegetation (coded 4 and colored green), [iv]most probably vegetation (coded 5 and colored green), [v]soil (coded 8 and colored red) and [vi]most probably soil (coded 9 and colored red). The classifier uses the signature statistics from the spectral signature database. It uses the mean, minimum and maximum values. The introduced classifier uses the minimum distance from the mean vector of the three classes of interest; water, vegetation and soil. If a pixel vector belongs to a certain class then the classifier checks if the pixel vector lies between the minimum and maximum vectors of that class. If so, the resulted class is certainly sure. Otherwise, the resulted class is most probably sure. For example, if the minimum distance for a pixel vector is close to the mean vector of vegetation then we have two cases. The first case; if the pixel vector lies between the minimum and maximum vectors of vegetation then the pixel is surly vegetation and coded 4 with green color but, the second case; if it is outside the range then it is most probably vegetation and coded 5 with green color (see Fig. 5). The introduced classifier was applied to all images of the study areas including images used to extract signatures and images that were left for testing the resulted signature for each study area. The results of the classification were

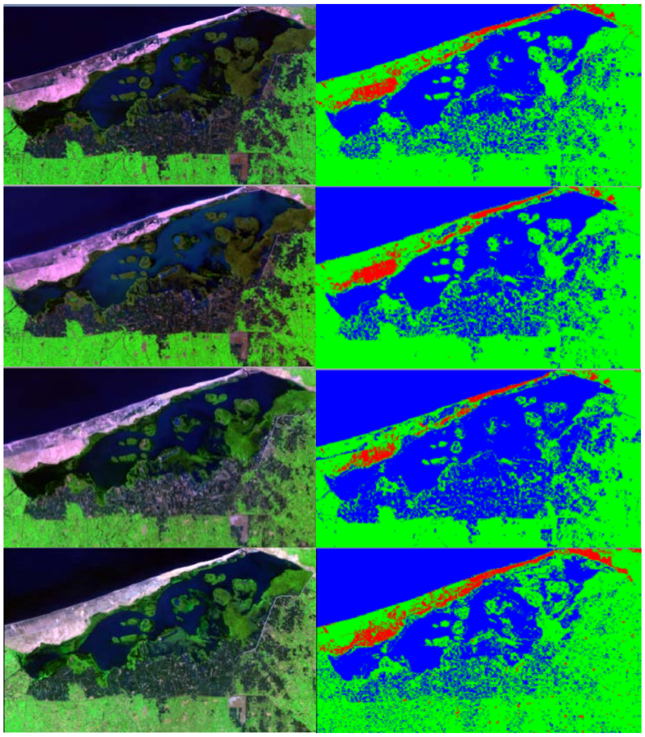

(a) *

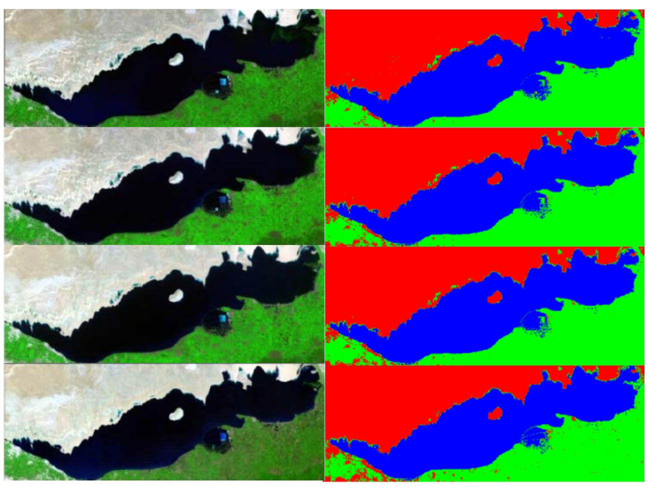

(b)

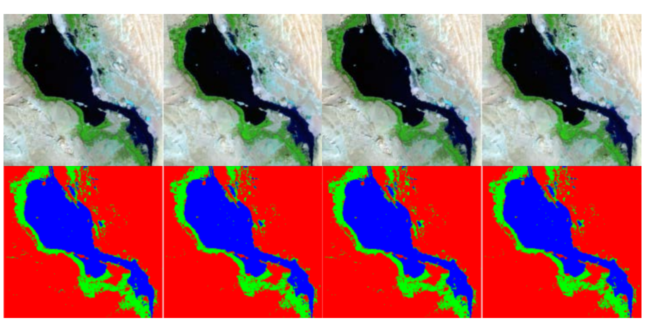

(c)

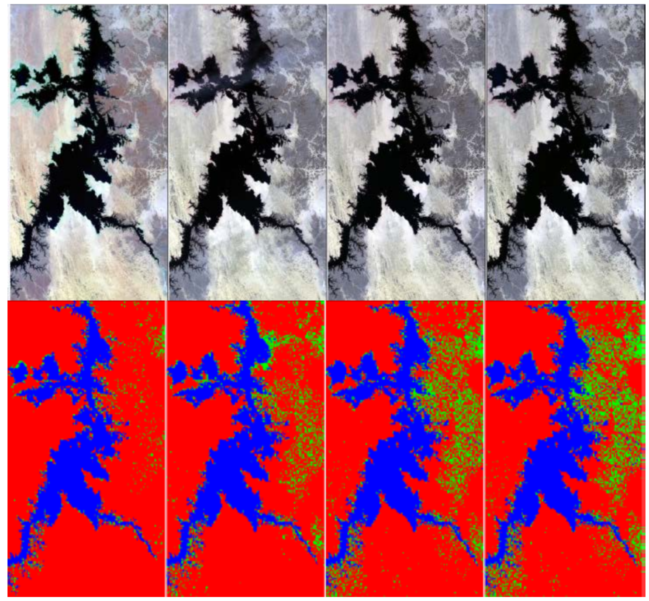

(d)

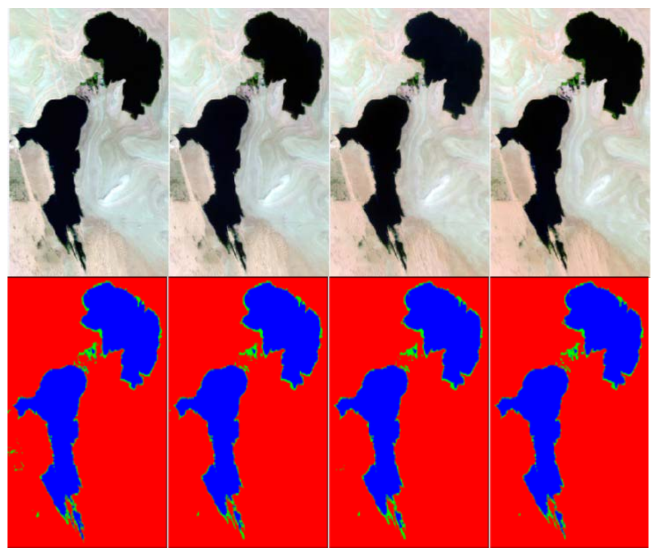

(e)

Fig. 11 Landsat ETM+ temporal series of the study areas and the corresponding classified images using the proposed classifier. The images are sorted from left to right or up to bottom according to date of acquisition (as in Table 1).
(a) Burullus Lake (b) Qaroun Lake (c) Nasser Lake
(d) Rayan Lakes (e) Morra Lakes

* It was found that the land bar area that lies between the Burullus lake northern shoreline and the Mediterranean Sea shoreline is not recognized totally as soil area but part of it recognized as vegetation because it is wetland area. Moreover the spectral profile of this bar tends to the vegetation profile not the soil profile which is tested by the Spectral Profile Viewer of ERDAS Imagine. This needs a comprehensive study.

compared to the supervised classification that uses the signature that was extracted from each image individually. Fig. 11 shows the classification results of the proposed classifier.

3.4 GUI Application

An ERDAS Imagine 2013 integrated GUI application was developed for the introduced classifier using ERDAS Macro Language (EML), ERDAS Spatial Modeler Language (SML) and ERDAS Graphical Modeler (GMD). The application was developed for Landsat 7 ETM+ classification that uses the spectral signature from the spectral signature database. The application can be extended to include other satellites and features. Fig. 11 shows the main window interface of the application. The user just enters the image to be classified in a form of a 6-bands reflectance .img file of Landsat 7 ETM+ and the output file is a 4-bit 1-band .img file. The signature data of Landsat 7 ETM+ is already entered from the signature database. If the user has updated values of the signature, he/she can just edit the new values.

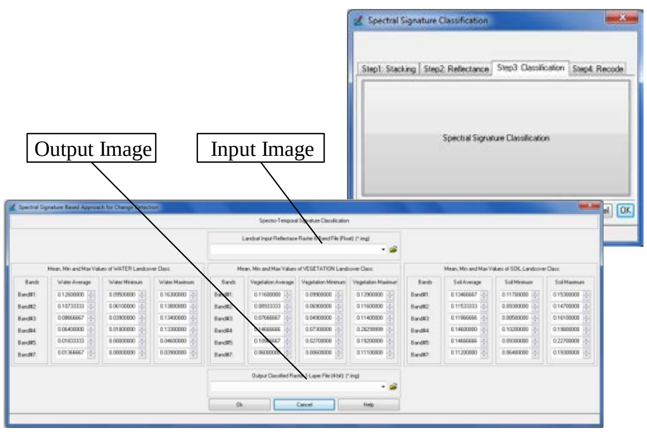

Fig. 12 An ERDAS Imagine 2013 integrated GUI application using ERDAS Macro Language (EML), ERDAS Spatial Modeler Language (SML) and ERDAS Graphical Modeler (GMD).

4. Results and Accuracy Assessment

Ground control points (GCP) have been randomly generated on the classified images that have been generated from the proposed classifier and from the unsupervised classifier that based on the minimum distance. The number of random points was stratified to the distribution of classes in the classified images (1GCP/15km^2 except for Nasser Lake 1GCP/75km^2 because of its huge area). Field verification beside local communities help has been conducted. Table 3 shows the image properties for each study area and the number of GCPs that was used for each study area.

Accuracy assessment is very important for understanding the developed results and employing these results for decision-making [10] [11]. The kappa statistic is also an assessment of whether a classification is correct or not. A kappa value close to one suggests that the classification is highly accurate and unlikely to be caused by chance, whilst a value of zero suggests the classification is no better than that which would be obtained randomly. Accuracy assessment has proven that the introduced classifier that uses the spectral signature gives nearly the same results of the supervised classification that uses the signature that was extracted from each image individually as shown in Table 4 as the correlation of the overall classification accuracy between both the proposed classifier and the supervised classifier gives a positive strong correlation of value 0.9947.

Table 3: The image properties for each study area and the number of GCPs that was used for each study area.

Study Area	*Width (Pixel)*	*Height (Pixel)*	*Total No° of Pixels*	*Area (Km^2)*	*No° of GCP*
Burullus	1822	1012	1843864	1497.68	100
Rayan	580	886	513880	417.40	28
Qaroun	1446	532	769272	624.84	42
Morra	1060	1019	1080140	877.34	59
Nasser	2650	4993	13231450	10747.25	144

Table 4: Accuracy assessments of the study areas for both the proposed classifier and the supervised classifier.

Study Area	**Serial** (as Table 1)	**Proposed Classifier**		**Supervised Classifier**	
		Overall Classification Accuracy	Overall Kappa Statistics	Overall Classification Accuracy	Overall Kappa Statistics
Burullus	1	86.00%	0.7502	86.00%	0.7243
	2	86.00%	0.7530	85.62%	0.7530
	3	86.00%	0.7472	86.00%	0.7472
	4	86.00%	0.7534	88.00%	0.7995
Qaroun	1	97.62%	0.9639	98.22%	0.9813
	2	97.62%	0.9640	97.62%	0.9640
	3	97.62%	0.9640	98.00%	0.9810
	4	95.24%	0.9278	95.00%	0.9251
Morra	1	94.92%	0.9013	95.00%	0.9026
	2	94.92%	0.8995	95.00%	0.9081
	3	94.92%	0.9013	95.00%	0.9026
	4	94.92%	0.8995	95.00%	0.9081
Nasser	1	85.24%	0.7502	85.24%	0.7502
	2	87.00%	0.8250	87.00%	0.8250
	3	85.90%	0.7792	85.90%	0.7792
	4	86.24%	0.7938	86.24%	0.7938
Rayan	1	96.43%	0.9141	96.21%	0.9015
	2	96.43%	0.9141	96.00%	0.9004
	3	96.43%	0.9141	97.00%	0.9162
	4	96.43%	0.9141	95.92%	0.9109

5. Conclusions and Future Work

Spectral signature of Landsat 7 ETM+ for the main classes of the earth; water, vegetation and soil were introduced. Temporal series of Landsat 7 ETM+ of five lakes located in Egypt were used as training areas to collect these signatures. A spectral signature database was developed to store these signatures in a standalone version using Microsoft Access 2013. However the spectral signature database was designed to store the spectral signatures for any other feature from any other satellite which needs an extra work and was leaved for future work research. The introduced classifier that uses the stored spectral signatures from the database gives a promising results for blind classification of any Landsat 7 ETM+ scene to classify the three classes; water, vegetation and soil. Results are nearly the same as the supervised classification that uses the same statistics of the signature. In fact, classifiers are generally sensitive to the high dimension of pixels. This is why the introduced classifier gives better results. Accuracy assessment has proven that, the introduced classifier gives better results than the supervised classification that uses signature from just one single image. The user needs not to find a signature for these classes. All what they need is to run the introduced classifier on the image to be classified.

It is supposed that any classifier that uses the proposed spectral signature should give better results than using the individual signature extracted from a single image that is to be classified. Moreover, it is supposed that, the more enhanced classifiers should give better classification results than the introduced classifier that based on the minimum distance classifier in its calculations. Future work can be summarized in the following points;

- Refining the spectral signatures.
- Break the signature of water into clear water, turbid water…etc. Break the signature of vegetation into dry grass, agriculture…etc. Break the signature of soil into mud, sand…etc.
- Filling in the database with more material spectral signatures, other than the three main features of the earth (water-vegetation-soil), for many other platforms especially for hyperspectral images that is future promising.
- Bands are equally used while signature extracting and classification. However, this is not always the best case. Some bands should be excluded and others should be weighted. This would be done after a comprehensive study for the feature of interest that is subject to signature extraction.
- Using better classifiers with the enhanced spectral signatures.
- C# Programming connection between the spectral signature database and the spectral signature GUI ERDAS Imagine 2013-application using ERDAS IMAGINE Developers' Toolkit v2013 and Microsoft Visual Studio 2010 (i.e. ODBC connection).

References

[1] ERDAS Field Guide, Norcross: ERDAS, Inc., December, 2010, pp. 566, 842-844.

[2] "Remote Sensing of the Environment," 1 December 2013. [Online]. Available: http://www.uwyo.edu/rs4111/lab03_reflectance_spectra_f13.pdf. [Accessed 1 December 2013].

[3] "USGS Spectroscopy Lab," U.S. Geological Survey, a bureau of the U.S. Department of the Interior, 20 6 2011. [Online]. Available: http://speclab.cr.usgs.gov. [Accessed 1 7 2013].

[4] P. COPPIN, I. JoNCKHEERE, B. NACKAERS and B. MUYS, "Assisted Change Detection, ERDAS Inc.," March 2004.

[5] G. Jianya, S. Haigang, M. Guorui and Z. Qiming, "A Review of Multi-Temporal Remote Sensing Data Change Detection Algorithms," *The International Archives of the Photogrammetry, Remote Sensing and Spatial Information Sciences,* vol. XXXVII. Part B7., p. 757, 2008.

[6] Remote Sensing, the image chain approach, vol. II, New York: Oxford University Press, Inc., 2007, p. 381.

[7] A. Akgün, A. Eronat and N. Turk, "Comparing Different Satellite Image Classification Methods: An Application In Ayvalýk District, Western Turkey," *XX th International Congress for Photogrammetry and Remote Sensing, Proceedings,* 2004.

[8] Campbell, Introduction to Remote Sensing, Luxemburg: European Commission, 2002, pp. 21-53.

[9] R. M. MaCoy, "Measurement of Vegetation, Soil and Water Bodies," in *Field Methods in Remote Sensing*, New York, The Guilford Press, 2005, pp. 71-114.

[10] T. M. Lillesand and R. W. Kiefer, Remote Sensing and Image Interpretation, 6th ed., New York: John Wiley and Sons, Inc., 2004, pp. 585-592.

[11] J. B. Campbel and R. H. Wynne, Introduction to Remote Sensing, 5th ed., New York: The Guilford Press, 2011, pp. 412-418.

Haitham Farouk received the B.S. and M.S. degrees in Computer Science from Ain Shams University and Helwan University in 1998 and 2005, respectively. During 1998-2007, he worked at Nature Conservation Sector (NCS), Egyptian Environmental Affairs Agency (EEAA) under the Cabinet of Ministers as a computer programmer. During 2007-2012, he was a Lecturer Assistant of Computer Science at Modern University for Technology & Information (MTI), Faculty of Computer Science, Department of Computer Science. He is now an IT & GIS national consultant for National Biodiversity Strategy and Action Plan (NBSAP) project under the Global Environment Facility (GEF) organization.